Kiwa rescues RecBCD for anti-phage activity

Thomas C. Todeschini[1], Yi Wu[1], Ameena Naji[1,2], Rupavidhya Mondi[1,3], Franklin L. Nobrega[1]*

[1]School of Biological Sciences, University of Southampton, SO17 1BJ Southampton, UK

*Corresponding author: F.Nobrega@soton.ac.uk

[2] Current address: School of Molecular and Cellular Biology, University of Leeds, Leeds LS2 9JT, UK

[3] Current address: The William Harvey Research Institute, Barts and The London School of Medicine, Queen Mary University of London, Charterhouse Square, London EC1M 6BQ, UK

Abstract

Bacteria have evolved numerous defence systems to combat phage infection, but our understanding of the underlying mechanisms is limited beyond their antiviral function. Here, we provide mechanistic insights into the Kiwa defence system, which is composed of two proteins, the transmembrane protein KwaA and the DUF4868 domain-containing protein KwaB. Using Kiwa from *Escherichia coli* ECOR8 and ECOR12, we found that KwaA detects phage infection by sensing inhibition of the host RNA polymerase. Consequently, the inhibitory effect of KwaA on the effector protein KwaB is relieved, which results in decreased phage DNA replication efficiency through a RecBCD-dependent pathway. Notably, Kiwa restores RecBCD activity even against phages that encode anti-RecBCD proteins. Our findings also reveal that KwaB has antiphage activity in the absence of both KwaA and phage trigger, but the conserved two-protein Kiwa operon implies that strict regulation of KwaB activity by KwaA is necessary to prevent potential auto-immunity.

Keywords: Kiwa, RNAP inhibitor, RecBCD, ATP depletion, phage DNA replication

Bacteria have evolved a set of mechanisms to defend against phage predation. Some of these defence mechanisms, such as CRISPR-Cas and restriction modification systems, have been widely studied and used in biotechnology, including Cas9-based gene editing[1]. However, most of the defence systems were discovered recently[2-10] and their molecular mechanisms are not well understood beyond their anti-phage functions. Research on some of these novel defence systems, such as BREX[5,11,12], DISARM[4,13,14], CBASS[15,16], Thoeris[17,18], Pycsar[19], PARIS[8], Gabija[3,20,21], Retrons[22], RADAR[6,23,24], DSR[25], Avast[6,26], Gasdermins[27], dCTP deaminase, dGTPase[28,29], and pVips[30], has made significant progress in elucidating their molecular activities. Further research is needed to fully characterise the dozens of defence systems that remain to be explored.

The Kiwa defence system is among the recent discoveries in anti-phage defence and is composed of two genes, *kwaA* and *kwaB*. *kwaA* encodes a protein with transmembrane-spanning abilities, while *kwaB* encodes a protein containing the DUF4868 domain of unknown function. The Kiwa system from *Escherichia coli* O55:H7 RM12579 was shown to protect against phages Lambda and SECphi18[3], but there is currently no further understanding of the precise mechanisms underlying the protective effects of Kiwa.

In this study, we demonstrate that Kiwa defence systems derived from *E. coli* ECOR8 and ECOR12 are activated by the inhibition of the host RNA polymerase (RNAP) by phage-encoded proteins. Upon sensing of RNAP inhibition, KwaA relieves its inhibitory activity on KwaB. KwaB then initiates a RecBCD-mediated process that reduces the efficiency of phage DNA replication, even in the presence of phage-encoded anti-RecBCD proteins. Notably, KwaB exhibits anti-phage activity

without the presence of KwaA and the phage trigger. However, the fact that KwaA and KwaB are present together in the conserved Kiwa operon across various bacterial species underscores the importance of tightly regulating KwaB activity through KwaA to avoid potential auto-immunity.

Results

Kiwa orthologues protect against different phages

To explore the diversity of Kiwa within prokaryotic genomes, we collected the Kiwa operons from all prokaryotic genomes accessible in the NCBI database. Out of the 198,640 genomes analysed, 1.6% were found to contain Kiwa operons, with the largest proportion (45%) being present in *Escherichia coli* (Supplementary Fig. 1a). This outcome aligns with the findings of earlier research[3].

By means of hierarchical cluster analysis of the KwaA and KwaB proteins within Kiwa operons, we observed their distribution into four clusters (Fig. 1a). For KwaA, we noted substantial diversity in protein size (ranging from 66 to 389 amino acids, Supplementary Table 1) and the number of transmembrane domains (varying from zero to five, with four being the most prevalent, Supplementary Fig. 1b). Previous research has demonstrated that diversity within defence systems of the same subtype may result in differing specificities of phage protection[2,15,17]. To determine whether diversity in Kiwa plays a role in defence specificity, we cloned five Kiwa systems from different clusters into *E. coli* BL21-AI (Fig. 1b, Supplementary Fig. 1c), which lacks these systems naturally. Infection assays with a panel of coliphages showed that four of the five Kiwa systems tested exhibited anti-phage activity with

phage specificity that was relatively consistent with the hierarchical clusters (Fig. 1a,c).

Moreover, the analysis of infection dynamics in liquid cultures confirmed that cells expressing Kiwa could protect against phage infection at both low (0.03) and high (3) multiplicities of infection (MOI). However, at higher MOI, we observed a delayed collapse of the culture, suggesting possible cell death (Fig. 1d, Supplementary Fig. 1d). Time post-infection assays demonstrated a decline in phage concentration within one hour of infection, revealing that the phage was capable of entering the cell but not replicating (Fig. 1e, Supplementary Fig. 1e).

To sum up, our findings reveal that Kiwa systems from different clusters exhibit distinct phage specificity patterns in terms of their protective efficacy.

KwaB is the effector of Kiwa and is regulated by an interaction with KwaA

Next, we investigated the role of individual genes for Kiwa's protective function by exposing single-gene deletions of Kiwa ECOR8 to phages. Our results indicate that the deletion of KwaB resulted in the loss of protection, whereas the deletion of KwaA had no effect (Fig. 2a, Supplementary Fig. 2a). Interestingly, the presence of KwaA in ECOR8 seems to induce cell toxicity, as evidenced by reduced cell growth in the absence of KwaB, but not in the absence of KwaA (Supplementary Fig. 2b). This toxic effect is also observed in Kiwa from ECOR49 and D9, but not in Kiwa from ECOR12 or SN82F48 (Supplementary Fig. 2b). KwaA contains transmembrane (TM) domains, which are also present in proteins of other characterised defence systems such as CBASS[15], Pycsar[19], and Retrons[22]. In CBASS, the deletion of the TM domains of the effector proteins abolished cell toxicity and revealed these to be essential for functionality[15]. To determine the role of the TM domains in KwaA-

induced cell toxicity, we truncated TM 1 (Δ5-25) and TM 1-2 (Δ5-74), resulting in reduced cell toxicity upon deletion of TM 1-2 (Supplementary Fig. 2b). Curiously, both truncations caused a loss of phage protection (Fig. 2a, Supplementary Fig. 2a). To further investigate the importance of the TM domains in Kiwa protection, we examined Kiwa SN82F48, which contains only two TM domains and does not provide phage protection (Fig. 1b). A closer inspection of the coding region of Kiwa SN82F48 revealed that the start of *kwaA* was located 336 nucleotides upstream of the annotated start, resulting in a longer open reading frame (ORF) that included four TM domains. The reconstitution of the longer *kwaA* restored the activity of Kiwa SN82F48 against two coliphages, providing evidence for the critical role of the four TM regions in KwaA for anti-phage defence (Fig. 2b, Supplementary Fig. 2c,d). Curiously, as with Kiwa ECOR12, no toxic effect on cell growth was observed (Supplementary Fig. 2b).

Based on the observation that protection is abolished only when a TM-truncated version of KwaA is present, and not when KwaA is completely absent, we hypothesized that KwaA and KwaB interact with each other, and that KwaB is in a free form in the cytoplasm when KwaA is absent, but bound to an inactive form of KwaA when this protein is present in a truncated version. To test our hypothesis, we conducted pull down assays with these proteins in *E. coli*. Since KwaA is a transmembrane protein and expression of such proteins is notoriously challenging, we opted to express only the cytoplasmic C-terminal region of KwaA (Supplementary Fig. 2e) that we suspect is responsible for the interaction with KwaB, and which is also essential for phage protection by Kiwa (Fig. 2a). By using the tagged C-terminal of KwaA we were able to pull down untagged KwaB, as confirmed by size exclusion

chromatography and mass spectrometry (Fig. 2c, Supplementary Fig. 3a), indicating that these two proteins interact.

Moreover, KwaB is characterised by the domain of unknown function DUF4868, which is present in a wide range of bacteria. A member of the family of DUF4868-containing proteins is involved in the synthesis of a bacteriocin toxin as part of a gene cluster, but the function of the domain itself remains unclear[31]. We show that point mutations on specific conserved amino acids within this domain (L145A/F147A and S272A, Supplementary Fig. 3b) result in decreased phage protection (Fig. 2a, Supplementary Fig. 2a). This supports the importance of the DUF4868 domain for phage defence by Kiwa. Alphafold[32] predictions suggest that KwaB can form dimers, and an interesting finding is that amino acid S272 may facilitate this dimerization by establishing several hydrogen bounds with the facing S272 amino acid in the second protein. Furthermore, amino acids L145 and F147 are contained within a beta strand that is situated in a pocket, suggesting a potential for these residues to interact with a target molecule (Supplementary Fig. 3c).

In summary, our results suggest that KwaB serves as the effector molecule for the Kiwa defence system, exhibiting anti-phage activity that is not reliant on KwaA. However, the activity of KwaB is modulated by its interaction with KwaA within the Kiwa operon.

KwaA senses phage host hijacking proteins to activate defence

We posited that the toxicity associated with some of the Kiwa systems tested was not a natural effect of the KwaA protein, but rather a consequence of overexpression of the membrane protein, which can be detrimental to the cell. To investigate this, we replaced the inducible T7 promoter in Kiwa ECOR8 with a constitutive Anderson

promoter that may aid in proper protein folding[33]. The results showed that Kiwa ECOR8 expressed under a constitutive promoter did not exhibit any toxicity (Fig. 3a). Sequencing of the plasmid and bacterial strain confirmed the absence of any genetic alterations (Supplementary Table 1), providing additional evidence that the toxicity observed previously in the absence of phage was likely caused by either overproduction or misfolding of KwaA.

Under the constitutive promoter, phage infection of Kiwa ECOR8 resulted in a delayed collapse of the culture, especially at high phage MOI, which may suggest an abortive infection phenotype[34] (Fig. 3a, Supplementary Fig. 4a). To further investigate this, we set out to identify the trigger of the defence system by evolving escape phages[35]. We observed that the Kiwa ECOR8 system expressed constitutively displayed a broader and stronger anti-phage activity compared to the same system expressed under the T7 inducible promoter (Fig. 3b, Supplementary Fig. 4b). Notably, the constitutively-expressed Kiwa exhibited particularly high activity against phage T3, with 10^4-fold protection (Fig. 3b) and decrease in plaque size (Fig. 3c, Supplementary Fig. 4c). Thus, we used phage T3 in our attempt to generate escape phages. Given the genomic similarities between T7Select (T7s) and T3, and the distinct patterns of protection provided against these phages by Kiwa ECOR8 (Fig. 3b), we included T7s in our efforts to generate escape mutants. We tested five T3 and three T7s mutants and observed that Kiwa from ECOR8 and ECOR12 lost protection against these mutant phages, suggesting that these systems from the same cluster (light blue, Fig 1a) use identical phage sensing mechanisms (Fig. 3d, Supplementary Fig. 5a). However, the phage escape mutants were unable to evade defence by Kiwa D9, from a different cluster (dark green, Fig. 1a), indicating that Kiwa systems from separate clusters employ different phage sensing mechanisms,

which likely account for the unique protective patterns we previously observed (Fig 1c).

The escape mutants were sequenced, revealing mutations (early stop codon or gene deletion) in the inhibitors of the stationary phase RpoS/σ^S sigma subunit of the host RNA polymerase (RNAP) (T7s gp5.7 and T3 T3p30)[36,37] (Fig. 3e, Supplementary Table 1). To confirm that the RNAP inhibitors trigger defence by Kiwa ECOR8, we expressed them in *trans* and observed the restoration of protective activity against the escape phages (Fig. 3f,g, Supplementary Fig. 5b,c). Despite the presence of mutations in the tail fibre gene of T7s (gp17) and T3 (T3p48), we observed that expression of the tail fibre in Kiwa cells did not have any impact on phage protection (Supplementary Fig. 5d).

The expression of the RNAP inhibitors caused a decrease in the cell growth of both Kiwa and control cells (Fig. 3g, Supplementary Fig. 5e), likely due to their effect on the bacterial RNAP. This limited our ability to test abortive infection using the trigger protein from the phage. In addition, we investigated whether Kiwa detected the RNAP inhibitor or the integrity of RNAP. Inspired by earlier work[29], we conducted experiments using rifampicin, a known inhibitor of bacterial RNAP, to assess its impact on the ability of the mutant phages to infect control and Kiwa cells. The findings demonstrated that in the presence of rifampicin, mutant phage propagation decreased in Kiwa cells compared to control cells, indicating that inhibition of the bacterial RNAP triggers Kiwa defence (Supplementary Fig. 5f). This suggests that the Kiwa defence system monitors the integrity of RNAP instead of directly sensing gp5.7/T3p30.

To determine which protein in Kiwa is responsible for sensing phage infection, we assessed the protective activity of Kiwa ECOR8 and its single gene mutants against the escape phages (Fig. 3h, Supplementary Fig. 5g). As expected, the escape phage was not inhibited by the complete Kiwa ECOR8 or ΔKwaB, but unexpectedly, ΔKwaA provided approximately 100-fold protection. These results indicate that the anti-phage activity of KwaB is independent of a phage trigger and suggest that KwaA is the protein responsible for sensing phage infection and modulating the effector KwaB.

To summarize, our findings indicate that KwaA senses RNAP inhibition by phage proteins. This recognition is likely responsible for releasing the effector protein KwaB, which is the key player in the Kiwa defence system.

RecBCD is required for Kiwa defence

To gain insight into the effector mechanism of Kiwa, we investigated different possible outcomes of the defence. We first tested whether Kiwa affects phage adsorption (Fig. 4a). Our results show that Kiwa from ECOR8 and ECOR12 does not affect the adsorption of T3 and T4 phages, suggesting that protection is provided at later stages of infection. As we observed a reduction in both extracellular and intracellular levels of viable phage (Fig. 4b), we next sought to determine if the decrease in intracellular phage particles was caused by reduced phage DNA replication. We extracted and sequenced DNA from control and Kiwa cells infected with phage at high MOI, both at the start and 30 minutes after phage infection, revealing a ≈25% decrease in phage DNA replication efficiency in Kiwa cells compared to control cells (Fig. 4c). This suggests that the defence system either

halts infection prior to the expression of phage proteins responsible for DNA replication, or acts directly on the phage DNA.

To test the former, we explored the possible abortive infection mechanism of Kiwa. As KwaA is a transmembrane protein, which can sometimes be associated with ATP secretion leading to cellular ATP depletion[38-41], we measured the ATP levels in control and Kiwa cultures infected with phage. Our results indicate that total ATP is depleted in phage-infected Kiwa cells (Fig. 4d), suggesting that both extracellular and intracellular ATP levels are reduced. This implies that ATP secretion is not involved and another intracellular process must be responsible for ATP consumption. Importantly, the depletion of ATP is not observed when either of the Kiwa proteins is absent (Fig. 4e). Given that KwaB alone is sufficient to provide anti-phage protection (Fig. 2a), our results indicate that ATP depletion is not the effector mechanism of Kiwa.

The phage RNAP inhibitors (gp5.7/T3p30) that trigger Kiwa defence are middle genes and are expressed during the same stage as the phage proteins involved in DNA replication[36,37,42]. This suggests that phage infection proceeds until this stage in Kiwa cells, leading us to hypothesise that the observed reduction in phage DNA replication is a direct consequence of a targeted action on phage DNA replication. As none of the Kiwa proteins are predicted to have nuclease activity, we investigated the possible involvement of host RecBCD in the Kiwa defence mechanism. RecBCD is known to be a crucial element of host immunity, with rapid nuclease activity on phage DNA[43,44]. This complex has been implicated in the activity of other defence systems, such as CRISPR-Cas[45] and prokaryotic Argonaute[46]. Thus, we hypothesized that Kiwa may mediate its defence through the RecBCD complex. To

test this hypothesis, we expressed the Kiwa system in a set of *E. coli* strains that had genomic deletions of the individual RecBCD genes and infected the cells with phage. Our findings show that RecBCD plays a critical role in Kiwa ECOR8 and ECOR12 defence, as the system becomes inactive against phage infection in its absence (Fig. 4f, Supplementary Fig. 6a). Curiously, RecD seems to play a more relevant role than RecB or RecC in Kiwa ECOR12, especially against phage T4.

Although RecD is known to possess ATP hydrolysis activity[47], its absence (or the absence of RecB or RecC) had no impact on ATP depletion in Kiwa cells during phage infection (Fig. 4g, Supplementary Fig. 6b). The fact that RecBCD is necessary for Kiwa protection but not for ATP depletion confirms that ATP depletion is not the effector mechanism of Kiwa and that it is more likely related to the interaction between KwaA and KwaB.

We hypothesized that KwaB may interact directly with RecD or RecBCD to activate the defence. However, when we expressed tagged KwaB in *E. coli* and tested for interaction with RecBCD proteins, none were pulled down with KwaB. During the SEC experiments aimed at identifying a potential interaction between KwaB and RecBCD, we observed that KwaB formed oligomers. This was evidenced by a shorter column retention time of the protein compared to when KwaB was co-expressed with the C-terminal of KwaA (Supplementary Fig. 4c). Mass spectrometry confirmed the presence of KwaB in all fractions. These findings suggest that the activation of KwaB may require oligomerization.

To further explore the interplay between KwaB and RecBCD in Kiwa defence, we assessed the level of protection provided by KwaB individually in cells with complete RecBCD or deleted individual genes. Our results indicate that KwaB provides full

protection only in the presence of complete RecBCD (Fig. 4h, Supplementary Fig. 6d), suggesting that KwaB and RecBCD work in concert to control phage infection.

Overall, our findings show that Kiwa defends against phage infection through a mechanism that involves activation of RecBCD by KwaB.

Discussion

In this study, we propose a mechanism for Kiwa defence that involves the activation of Kiwa through the inhibition of host RNAP by phage-encoded proteins, ultimately resulting in a RecBCD-dependent control of phage DNA replication (Fig. 4i).

We used phage mutants that escaped defence to identify the activators of Kiwa ECOR8 and ECOR12 defence, which were found to be the inhibitors of *E. coli* RNAP σ^s of phages T7s (gp5.7) and T3 (T3p30). Additional experiments using a transcription inhibitor, rifampicin, established that Kiwa detects the inhibition of host RNAP instead of the phage proteins. This is consistent with the observation that other defence system, such as dCTP deaminase, dGTPase, AVAST type III, and *toxIN*[29,35,48], also sense phage infection via binding to RNAP inhibitor or guarding the integrity of the host RNAP function, indicating that this is a common strategy employed by multiple defence systems. Interestingly, the phage-encoded RNAP inhibitor that activates Kiwa from ECOR8 and ECOR12 does not activate Kiwa from *E. coli* D9, suggesting that distantly related Kiwa operons are activated by different triggers, resulting in their distinct anti-phage specificities.

Complementation assays in *trans* showed that the RNAP inhibitor proteins activate Kiwa defence only when the full system (KwaA+KwaB) is present, while KwaB alone is capable of providing anti-phage defence in the presence or absence of the phage-

encoded RNAP inhibitor. Because of this we propose that KwaA is the protein responsible for sensing phage infection in Kiwa.

Sensing of host RNAP inhibition by KwaA likely controls the activity of KwaB, which we found to bind to the C-terminal of KwaA. However, when we deleted the C-terminal of KwaA, protection was abolished, even though KwaB should be active in the cytosol. We hypothesise that some other part of KwaA interacts with KwaB and limits its activity, mostly likely the 20 amino acids of KwaA predicted to be cytosolic (G75-F94). Moreover, analysis of the ATP levels in Kiwa cells revealed that the interaction between KwaA and KwaB results in a reduction of ATP. However, this ATP depletion is not linked to the protective function of KwaB and is not considered the effector mechanism of Kiwa. Instead, we suggest that the interaction between the Kiwa proteins or between these proteins and the trigger may cause the observed ATP depletion.

KwaB contains the DUF4868 domain, which is commonly found in the human gut microbiome. A homologue of this domain from *Lactobacillus casei* CRL 705 is involved in the biosynthesis of a bacteriocin toxin[31]. The specific function of this domain remains unknown, but its conservation across different KwaB homologues and the loss of protection upon key amino acid substitutions suggests its significance for anti-phage defence. Our study demonstrates that KwaB, with or without KwaA, facilitates phage defence through a RecBCD-dependent mechanisms that hinders the efficiency of phage DNA replication. Although pull-down assays with tagged KwaB expressed in *E. coli* did not reveal any direct stable interaction between KwaB and RecBCD proteins, this interaction may be transient or weak, or the effect may be indirect. Notably, the protective effect of RecBCD is only observed in the presence of

KwaB, regardless of whether KwaA is present or not. Other defence systems have also been shown to work alongside RecBCD, such as the CRISPR-Cas systems that uses DNA fragments created by RecBCD to acquire new spacers targeting phages[45,49], and the Retron Ec48 system that guards RecBCD activity and prompts abortive infection upon inhibition of this complex by phage-encoded proteins[22]. The mechanism of RecBCD dependence in Kiwa appears to be distinct from other defence systems and uses the inherent anti-phage properties of RecBCD. It is relevant to note that phage-encoded inhibitors of RecBCD do not seem to affect Kiwa's defence mechanism, as protection against phages T4, T3, and T7s is observed regardless of their encoded inhibitors (gp2, T3p31, and gp5.9, respectively). This suggests that Kiwa can restore the RecBCD activity towards these phages, either by directly modulating its activity or by preventing the RecBCD inhibitors from affecting RecBCD.

While we could not definitively confirm that Kiwa results in an abortive infection phenotype, we propose that this is the case at least against phages that cause host DNA degradation. Phages T3, T7, and T4 use nucleases that rapidly degrade the bacterial host chromosome at the early stages of phage infection[50,51]. As Kiwa senses phage infection by detecting phage-encoded RNAP inhibitors expressed at the middle stage of the phage infection cycle[36], it is likely that the host chromosome is damaged beyond repair by the time the defence mechanism kicks in. Therefore, RecBCD activity may result in degradation of phage DNA, but will not be adequate to save the cell infected with phages that degrade the host chromosome. Additionally, the fact that KwaB can provide protection in the absence of KwaA, but is still present with KwaA in operons, implies that KwaB might be toxic and that its activity needs to be regulated for cell survival. While our assays showed no evidence of a toxic effect

of KwaB on the cells, it is possible that the RecBCD-mediated action of KwaB could have harmful effects on the cells in the long term, such as increased mutation rates.

Altogether, our findings reveal a new mechanism for defence against phages in which Kiwa proteins reinstate RecBCD activity to regulate phage DNA replication, independent of the presence of phage-encoded RecBCD inhibitors.

Methods

Bacterial strains and phages

E. coli Dh5α, and BL21-AI, BL21-AIΔRecB, BL21-AIΔRecC, and BL21-AIΔRecD[45] were grown at 37 °C in Lysogeny Broth (LB) for liquid cultures or LB agar (LBA, 1.5 % (w/v) agar) for solid cultures. Whenever applicable, LB was supplemented with chloramphenicol (25 µg/mL), spectinomycin (50 µg/mL), Isopropyl ß-D-1-thiogalactopyranoside (IPTG, 1 mM) or L-Arabinose (0.2 %), to ensure maintenance of plasmids or induce protein expression. Phage infection was performed in LB at 37 °C. Phages were propagated by infecting *E. coli* BL21-AI grown to an optical density at 600 nm (OD_{600}) of 0.2-0.4 with 5-10 µL of a phage lysate. Infected cultures were grown for at least 4 hours or until culture collapse. The culture was then centrifuged at 11,000 × *g*, 4 °C for 15 min to remove cell debris, and the supernatant was filter sterilized through a 0.22 µm filter. All strains and phages used in this study are listed in Supplementary Table 2.

Plasmid and strain construction

Kiwa systems from *E. coli* ECOR8, ECOR12, ECOR49, and D9 were amplified by Q5 polymerase (New England Biolabs) using primers indicated in Supplementary

363 Table 3. Kiwa from *Ralstonia mannitolilytica* SN82F48 was ordered synthetically as a
364 gBlock (Integrated DNA Technologies) (Supplementary Table 3). Kiwa systems were
365 cloned into pACYCDuet-1 (Novagen EMD Millipore) by restriction enzyme cloning or
366 Gibson assembly (NEBuilder Hifi DNA assembly Master Mix). When appropriate,
367 deletions, mutations and truncations of Kiwa operons were engineered by around-
368 the-horn PCR with primers listed in Supplementary Table 3. A plasmid with Kiwa
369 ECOR8 under a constitutive promoter (pUOS023) was constructed by substitution of
370 the T7 promoter and lac operator of pUOS017 with the constitutive Anderson
371 promoter J23104 (http://parts.igem.org/Promoters/Catalog/Anderson)[33]. For protein
372 purification, KwaA and KwaB genes of ECOR8 were cloned into the 13S-S plasmid
373 (Berkeley MacroLab) under an inducible T7 promoter, with a 6X His SUMO TEV N-
374 terminal tag. 13S-S ECOR8 KwaA C-terminus was constructed by around-the-horn
375 PCR on pUOS025. GFP was amplified from pARACDF (Addgene 47516) and phage
376 proteins gp5.7/T3p30 and gp17/T3p48 were amplified from the genome of T7s or T3
377 respectively using the primers indicated in Supplementary Table 3. These proteins
378 were cloned into pCDF1-b (Novagen) under the control of a T7 promoter. All
379 plasmids were transformed into *E. coli* Dh5α, extracted using the GeneJET Plasmid
380 Miniprep kit (Thermo Fisher), verified by Sanger sequencing (Eurofins Genomics)
381 and transformed into electrocompetent *E. coli* BL21-AI. Plasmids built for this study
382 are listed in Supplementary Table 4.

383 **Plaque assays**

384 Phages were ten-fold serially diluted in LB and spotted on soft agar plates (0.7 %
385 (w/v) agar) of *E. coli* BL21-AI containing a control plasmid or individual Kiwa
386 systems. For inducible systems, overnight cultures were diluted 1:50 in LB with 0.2

% L-arabinose and 1 mM IPTG, and grown for 4 hours at 37 °C with agitation before preparing bacterial lawns for spot assays. For spot assays in strains expressing phage proteins *in trans*, induction was performed on plate by supplementing soft agar with L-arabinose and IPTG. Plates were left to dry at room temperature and incubated overnight at 37 °C. Plaque forming units (PFUs) were determined by counting the plaques after overnight incubation. Whenever plaques were too small to be counted, a clear lysis area was set to be equal to 100 PFUs. Fold defence was determined by calculating the ratio of phage concentration of Kiwa expressing strain in relation to control strain. Difference in phage plaque size produced in a Kiwa strain relative to a control was determined by measuring the plaque area of 100 individual plaques of phages T3, T4, T7, NBG2 and S1-BL21L.

Turbidity assays

Overnight bacterial cultures of *E. coli* BL21-AI with a control plasmid or individual Kiwa systems were diluted 1:100 in LB, supplemented with L-arabinose and IPTG if required, and grown at 37 °C with agitation until cultures reached an OD_{600} of ≈0.3. Cultures were normalized to an OD_{600} of 0.1 and dispensed in a 96-well plate. Growth was monitored every 10 min in a ClarioStar plus plate reader at 37 °C with agitation. When OD_{600} reached ≈0.3, cells were either kept uninfected or infected with phage at the desired MOI. Growth was then monitored for 500 min post infection. For cells expressing phage proteins *in trans*, L-arabinose (0.2%) and ITPG (1 mM) were added simultaneously with the phage.

Time post infection assays

Overnight bacterial cultures of *E. coli* BL21-AI with a control plasmid or individual Kiwa systems were diluted 1:100 in LB medium, supplemented with L-arabinose (0.2

%) and IPTG (1 mM), and grown at 37 °C with agitation until an OD_{600} of ≈0.3. Cultures were normalized and infected with phage T3 or T4 at an MOI of 3. At 0, 60 and 90 min post infection, a sample was taken, serially diluted, and phages were quantified by plaque assay on a phage-sensitive bacterial lawn (*E. coli* BL21-AI + pUOS016). PFUs were counted after overnight incubation at 37 °C.

Adsorption assays

Overnight bacterial cultures of *E. coli* BL21-AI with a control plasmid or individual Kiwa systems were diluted 1:100 in LB medium, supplemented with L-arabinose (0.2 %) and IPTG (1 mM), and grown at 37 °C with agitation until an OD of ≈0.3. Then, 500 µL of bacterial culture were infected with phage T3 or T4 at an MOI of 0.005, and incubated for 15 min at 37 °C with agitation. A sample was taken and serially diluted to obtain the total phage concentration. Subsequently, cells were centrifuged (8,000 × *g*, 1 min) and a sample from the supernatant was taken and serially diluted to obtain the non-adsorbed phage concentration. Dilutions were spotted on a phage-sensitive bacterial lawn (*E. coli* BL21-AI + pUoS016). The concentration of adsorbed phages was determined by subtracting non-adsorbed phage concentration from the total phage concentration. The percentage of adsorbed phages was calculated as the ratio between adsorbed and total phages.

Intra- and extracellular phage concentrations

Overnight bacterial cultures of *E. coli* BL21-AI with a control plasmid or Kiwa ECOR8 were diluted 1:100 in LB medium, supplemented with L-arabinose (0.2 %) and IPTG (1 mM), and grown at 37 °C with agitation until cultures reached an OD_{600} of ≈0.3. Cultures were normalized and infected with phage T4 at an MOI of 10^{-5}. At 90 minutes post infection a sample was taken and centrifuged (8,000 × *g*, 1 min, 4 °C).

The supernatant was serially diluted to obtain the extracellular phage concentration. The remaining supernatant was discarded and the cell pellet was washed once with ice cold LB and harvested by centrifugation (8,000 × *g*, 1 min, 4 °C). The supernatant was discarded and the cell pellet was re-suspended in ice cold LB, after which a 1:1 volume of chloroform was added. The sample was mixed by vortexing, and the aqueous layer was extracted after centrifugation (8,000 × *g*, 5 min, 4 °C) and serially diluted to obtain the intracellular phage concentration. Dilutions were spotted on a phage-sensitive bacterial lawn (*E. coli* BL21-AI + pUOS016), and the PFUs were counted after overnight incubation at 37 °C.

DNA replication assay

Overnight bacterial cultures of *E. coli* BL21-AI with a control plasmid or individual Kiwa systems were diluted 1:100 in LB medium, supplemented with L-arabinose (0.2 %) and IPTG (1 mM), and grown at 37 °C with agitation until cultures reached an OD_{600} of ≈0.3. Cultures were normalized and infected with phage T3 or T4 at an MOI of 3. At 0 and 30 min post infection, a 5 mL sample was taken and centrifuged (15,000 × *g*, 5 min, 4 °C). The cell pellets were snap frozen using liquid nitrogen and stored at -80 °C. Total DNA was extracted using the GeneJET Genomic DNA Isolation kit (Thermo Fisher), using the Gram-negative protocol. Samples were sequenced at SeqCenter (Pittsburgh, PA, USA), where sample libraries were prepared using the Illumina DNA Prep kit and IDT 10bp UDI indices, and sequenced on an Illumina NextSeq 2000, producing 2x151bp reads. Demultiplexing, quality control and adapter trimming was performed with bcl-convert (v3.9.3). Reads were aligned to *E. coli* BL21-AI and phage T3 or T4 reference genomes (CP047231, NC_003298 and NC_000866) using MiniMap2[52] in Geneious prime 2023.0.1. Replication efficiency was determined by calculating the increase of phage genomes

to the number of cells at time 0. The percentage was calculated by comparison of Kiwa infected cells to control cells over time.

RecBCD mutant assays

Strains with individual deleted RecBCD subunits were transformed by electroporation with a control plasmid or individual Kiwa systems and recovered on LBA supplemented with kanamycin (50 µg/mL). Colonies were picked and grown overnight at 37 °C. Spot assays were performed with Phage T3 and T4 as described above for inducible systems.

ATP assays

Overnight bacterial cultures of *E. coli* BL21-AI, or *E.coli* BL21-AI ΔRecB , ΔRecC or ΔRecD with a control plasmid or individual Kiwa systems were diluted 1:100 in LB medium, supplemented with L-arabinose (0.2 %) and IPTG (1 mM), and grown at 37 °C with agitation until an OD_{600} of ≈0.3. Cultures were normalized and either kept uninfected or infected with phage T3 or T4 at an MOI of 3 or 0.03. At 0 and 30 min post infection a sample was taken and serially diluted, and ATP concentration was determined by following the BacTiterGlo cell viability kit protocol (Promega). Luminescence was measured in ClarioStar plus plate reader at room temperature. ATP levels of Kiwa expressing cells were compared to control cells at 0 and 30 min post infection.

Isolation and sequencing of escape phages

Escape phages were isolated by picking single plaques at the lowest dilution of a spot assay on a lawn of *E. coli* cells expression Kiwa ECOR8 under a constitutive promoter. The resistant phenotype of each escape phage was determining by comparing the EOP of the escape phage to the EOP of the wild type phage in the

presence of Kiwa ECOR8. Isolated phages were further propagated by infecting a liquid culture of Kiwa ECOR8 as described above. Phage lysates were pelleted following the NaCl/PEG8000 precipitation protocol as previously described[53]. The phage pellets were re-suspended in LB, and treated with DNase I and RNase A (1 µg/mL each) for 30 min at room temperature. EDTA (20 mM), proteinase K (50 µg/mL) and SDS (0.5%) were added to the suspension and incubated overnight at 56 °C. DNA was extracted using the Zymo Clean & Concentrator-5 kit (Zymo Research). Samples were sequenced at SeqCenter (Pittsburgh, PA, USA), where sample libraries were prepared using the Illumina DNA Prep kit and IDT 10bp UDI indices, and sequenced on an Illumina NextSeq 2000, producing 2x151bp reads. Demultiplexing, quality control and adapter trimming was performed with bcl-convert (v3.9.3). Mutations were identified by mapping sequencing reads to the respective reference phage genomes (NC_003298 for T3 and Supplementary Table 1 for T7s) using Breseq[54] v0.37.0 with default parameters. Only mutations that occurred in the isolated mutant but not in the wild type phage were considered. Silent mutations within protein-coding regions were also neglected.

Rifampicin assay

Overnight bacterial cultures of *E. coli* BL21-AI or BL21-AI ECOR8c were diluted 1:100 in LB medium and grown at 37 °C with agitation until an OD600 of ≈0.3. Cultures were infected with phage T3 mutant n.2 at an MOI of 0.6 and treated with Rifampicin (100 µg/mL) or kept untreated. At 0, 30, 60, and 90 min post infection a sample was taken and serially diluted. Phages were quantified by plaque assay on a phage-sensitive bacterial lawn (*E. coli* BL21-AI + pUOS022), and the PFUs were counted after overnight incubation at 37 °C.

Bacterial growth upon induction of phage trigger

Overnight cultures of *E. coli* BL21-AI ECOR8c or a control with a plasmid encoding phage T3 gp30 were normalised to an OD_{600} of 1.0. Normalised cultures were serially diluted in LB and spotted onto LBA plates with or without L-arabinose (0.2 %) and IPTG (1 mM)). Plates were incubated overnight at 37 °C for colony forming units (CFU) counting.

Protein expression and purification

Overnight cultures of *E. coli* BL21-AI with His-SUMO-TEV::ECOR8 KwaA C-terminus and ECOR8 KwaB, or His-SUMO-TEV::ECOR8 KwaB with mVenus YFP as a control were diluted in LB and grown at 37 °C with agitation until an OD_{600} of ≈0.4. Grown cultures were incubated on ice for 1 hour and protein expression was induced with L-arabinose (0.2 %) and IPTG (1 mM), followed by overnight incubation at 20 °C and 150 rpm. The overnight cultures were harvested by centrifugation (8,000 × g, 30 min, 4 °C). The supernatant was discarded and the cell pellets were re-suspended in lysis/wash buffer (50 mL per 1 L of initial culture, 100 mM Tris-HCl, 150 mM NaCl, 1 mM DTT, 5% glycerol, 25 mM imidazole, pH 7.5) supplemented with Pierce™ Protease Inhibitor Tablets EDTA-free (Thermo Fisher). Cell lysis was performed three times in a cooled French press (15Gpa). The cell lysate was centrifuged (17,000 × g, 30 min, 4 °C) and debris were removed by filtration (0.45 µm PES). The filtered supernatant was incubated with HisPur™ Ni-NTA Resin (Thermo Fisher) (500 µL/50 mL lysate) pre-washed with 20 mL of lysis/wash buffer for 30 min at 4 °C. The sample was loaded onto a 5 mL Pierce™ Disposable Column (Thermo Fisher) for gravity-flow affinity chromatography. The column was washed with 15 mL of ice-cold lysis/wash buffer, and the protein was eluted with ice-cold elution buffer (100

mM Tris-HCl, 150 mM NaCl, 1 mM DTT, 5% glycerol, 250 mM imidazole, pH 7.5). Pooled fractions were concentrated (Amicon Centrifugal concentrator with Ultracel membrane, 3 kDa MWCO), and the buffer exchanged to running buffer (100 mM Tris-HCl, 150 mM NaCl, 1 mM DTT, 5% glycerol, pH 7.5). The resulting protein sample was subjected to size exclusion chromatography using a Superdex 200 increase 10/300 GL (Cytiva) column equilibrated with running buffer with 0.5 mL/min flow rate using running buffer as a mobile phase. Fractions of interest were analysed by SDS-PAGE, snap frozen in liquid nitrogen and stored at -80 °C until further use. Fractions containing protein brands corresponding to the size of tagged KwaA C-terminus, tagged KwaB or KwaB were analysed by mass spectrometry as detailed below.

Protein identification by mass spectrometry

The proteins in the purified fractions were analysed by mass spectrometry at the Mass Spectrometry Facility of the Department of Biotechnology at Delft University of Technology (Netherlands), as previously described[55]. Briefly, proteins were identified following in-solution digestion, or after SDS-PAGE analysis followed by in-gel digestion. In solution digestion was performed by mixing 100 µL of each protein solution with 440 µL of 200 mM ammonium bicarbonate buffer (ABC). To this solution, 30 µL of 10 mM dithiothreitol (DTT) solution was added, and incubated at 37 ˚C, 300 rpm for 1 hour. Next, 30 µL of 20 mM Iodoacetamide (IAA) solution was added and incubated in the dark, at room temperature, for 30 minutes. 5 µL of Trypsin solution (0.1 µg/µL) were added to the solution, and the solution was incubated at 37°C, 300 rpm overnight. Samples were desalted and cleaned using solid phage extraction and dried afterwards. The dried samples were resuspended in

15 µL 3% acetonitrile in water plus 0.1 % formic acid under careful vortexing. An aliquot corresponding to approximately 100 ng protein digest was analysed using a nano-LC EASY 1200 (Thermo Scientific, Germany) coupled online to a QE plus Orbitrap mass spectrometer (Thermo Scientific, Germany), which was operated in data-dependent acquisition (DDA) mode, acquiring MS2 spectra of the top 10 peptide signals. Mass spectrometric raw data were analysed using PEAKS Studio X (Bioinformatics Solutions Inc., Canada) by comparing fragmentation spectra to a database consisting of the target protein sequences and the *E. coli* BL21 AI proteome (NCBI). Database searching was performed allowing 20 ppm parent mass error, 0.2 Da fragment mass error, 2 missed cleavages, carbamidomethylation as fixed, and oxidation and deamidation as variable peptide modifications. Peptide matches and protein identifications were filtered for 1% false discovery rate. Protein identifications with >1 unique peptide sequences were considered as confident matches.

Bioinformatic analysis

All prokaryotic genomes were retrieved from NCBI, and Kiwa containing genomes were identified using the Prokaryotic Antiviral Defense LOCator (PADLOC)[10]. Only complete Kiwa systems that contained at least one KwaA and one KwaB gene within the operon, were considered for further analysis (Supplementary Table 5). KwaA and KwaB protein sequences were aligned using Clustal Omega[56] with default parameters and the noise was removed with CIAlign[57]. The multiple sequence alignment was used on IQ-tree[58] to generate a tree with -alrt 1500, -bb 1500 parameters, followed by masking of regions with non-homologous adjacent characters using prequal. iTOL[59] was used for tree visualisation. Protein domains of KwaA and KwaB were identified using HHpred[60]. Transmembrane domains were

identified using DeepTMHMM[61], and protein size was predicted using the ProtParam webtool[62]. Sequence alignments of KwaA C-terminus and KwaB were computed by Clustal Omega[56] and visualised using Geneious Prime v2023.0.1. For KwaB mutants, a total of nine homologs present in the KwaB ECOR8 and ECOR12 cluster were selected and aligned to determine amino acid conservation.

Statistical analysis

Unless stated otherwise, experiments were performed in biological triplicates and are represented as the mean and standard deviation. Statistical significance was calculated by ration paired t-test or by two-way ANOVA with sidak's multiple comparison test, with a significance level of 0.05.

Data availability

All data supporting the findings of this study are available within the paper and in the Supplementary Data. Raw data is available from Figshare via the following DOIs: Sequencing reads of phage escape mutants https://doi.org/10.6084/m9.figshare.21652433.v1, sequencing reads of phage infection of Kiwa cells https://doi.org/10.6084/m9.figshare.21648587.v1, sequencing reads of ECOR8c https://doi.org/10.6084/m9.figshare.22093256.v1, and mass spectrometry data https://doi.org/10.6084/m9.figshare.22147931.v1. All unique bacterial strains, phages, and plasmids generated in this study are available from the corresponding author upon request.

Acknowledgements

We thank Morgen Hedges for bacteriophage illustrations, Cristian Aparicio-Maldonado for helping with protein purification, and Dita Heikens and Martin Pabst from TU Delft for the mass spectroscopy analysis. This work was supported by grant RGS\R2\222312 from the Royal Society to F.L.N.

Author contributions

Conceptualization, F.L.N.; Methodology; T.C.T. and F.L.N.; Formal Analysis, T.C.T., F.L.N.; Investigation, T.C.T., Y.W., A.N., and R.M.; Visualization, T.C.T.; Data Curation, T.C.T., Y.W., F.L.N.; Writing – Original Draft, T.C.T., F.L.N.; Writing – Review & Editing, F.L.N.; Resources, F.L.N.; Funding Acquisition, F.L.N..

Declaration of interests

The authors declare no competing interests.

Figure legends

Fig. 1: Kiwa orthologues provide defence against multiple coliphages. a Clustering of KwaA (left) and KwaB (right) homologues in prokaryotic genomes. The tree was built using only non-redundant sequences. Each cluster is identified by a specific colour shading. The tree includes annotations for Kiwa operons that were tested in this study, and any Kiwa operons that have previously been confirmed to provide anti-phage activity are indicated with a shield symbol. **b** Schematic representation of the Kiwa operons tested in this study, obtained from *Escherichia coli* (ECOR8, ECOR12, ECOR49, D9) and *Ralstonia mannitolilytica* (SN82F48) strains. TM, transmembrane domain. DUF, domain of unknown function. **c** Anti-phage activity of five Kiwa operons shown as fold protection of efficiency of platting assays. m, plaque morphology change relative to a control strain expressing mVenusYFP. **d** Growth curves of Kiwa ECOR12 or control cells infected by phage T4 at an MOI of 3 or 0.03. Data shows the mean of three biological replicates. **e** Effect of Kiwa ECOR8 (left) and ECOR12 (right) on phage propagation. Data represents plaque forming units (PFU) per mL (PFU/mL) of phage T4 at different time points post infection of Kiwa or control cells. Asterisks mark statistically significant PFU/mL decreases relative to a control (Two-way ANOVA, $p < 0.05$). Bar graphs represent the average of 3 biological replicates with individual points overlaid.

Fig. 2: Transmembrane domains of KwaA and DUF4868 domain of KwaB are essential for the anti-phage activity by Kiwa. a Impact of deletions, truncations and point mutations on the ability of Kiwa ECOR8 to defend against phages T3 and T4. The domain organisation of Kiwa ECOR8 is shown on top, with transmembrane (TM) domains of KwaA in dark green, C-terminal domain of KwaA, in light green, and

point mutations in the DUF4868 domain of KwaB in orange. The fold defence was calculated by dividing the number of PFU (plaque-forming units) per mL of control and Kiwa strains. Asterisk indicate a statistically significant decrease in defence compared to Kiwa ECOR8 (Two-way ANOVA, $p < 0.05$). The bars represent the average of two biological replicates with individual data points overlaid. **b** Effect of reconstituing two TM domains of KwaA on the defensive activity of SN82F48 against phages T3 and T7s. A schematic of the SN82F48 operon with added TM domains in green is shown on top. The fold defence was calculated as the ratio of PFU/mL on control and Kiwa strains. Asterisks indicate a statistically significant decrease in defence compared to truncated SN82F48 (Two-way ANOVA, $p < 0.05$). The bars represent the average of two biological replicates with individual data points overlaid. **c** Pulldown assay of ECOR8 KwaA C-terminus and KwaB. The KwaA C-terminus was N-terminally tagged with a HIS-Sumo-TEV tag and co-expressed with KwaB. A schematic of the heterologous expression system used for protein overexpression is shown on top. The size exclusion chromatogram shows absorbance at 280 nm on the left, with elution volume corresponding to the peak run on SDS-PAGE on the right.

Figure 3. Kiwa is activated upon detecting inhibition of host RNA polymerase. **a** Growth curves of *E. coli* with Kiwa ECOR8 under expression of a constitutive promoter (ECOR8c) or control cells infected with phage at MOI of 3 or 0.03. Lines show the mean of three biological replicates. **b** Kiwa ECOR8c exhibits increased defence against three phages in comparison to ECOR8 (T7 inducible promoter). The data represents fold defence in relation to control cells, and it is the average of two biological replicates. Plaque morphology change compared to control is indicated by

669 “m”. **c** Effect of ECOR8c on plaque size of infecting coliphages. The data represents
670 plaque sizes of phages infecting ECOR8c cells relative to the average size of
671 plaques on controls cells. Asterisks indicate a statistically significant decrease in
672 plaque size in Kiwa cells compared to the control strain (Two-way ANOVA, $p < 0.05$).
673 The mean of 100 replicates is shown, with individual points overlaid. **d** Reduction of
674 defence by Kiwa ECOR8, ECOR12 or D9 when infected by phage escape mutants
675 (n.1-n.5). Fold defence is calculated as the ratio of PFU/mL on Kiwa and control
676 strains. The average of two biological replicates is shown, with individual data points
677 overlaid. Asterisks indicate a statistically significant decrease in defence compared
678 to control (Two-way ANOVA, $p < 0.05$). **e** Mutations in gp5.7 of phage T7s and T3p30
679 of phage T3 allow evasion of Kiwa defence. Phages with complete deletions of gp5.7
680 or T3p30 are annotated separately. The full list of mutations and deletions in the
681 escape mutants is detailed in Supplementary Table 2. **f** Reconstitution of gp5.7 and
682 T3p30 recovers ECOR8c defence activity against phage escape mutants. Fold
683 defence was calculated as the ratio of PFU/mL in Kiwa and control. Asterisks
684 indicate a statistically significant increase of defence in relation to a control of
685 ECOR8c-GFP (Ratio paired t-test, $p < 0.05$). The bars represent the mean of two
686 biological replicates, with individual data points overlaid. **g** Growth curves of *E. coli*
687 Kiwa ECOR8c expressing T3p30, gp5.7 or GFP (control) infected with phage escape
688 mutants at an MOI of 0.6 or 0.06. The curves represent the mean of three biological
689 replicates. **h** Effect of deletion of Kiwa genes on the infectivity of phage escape
690 mutants. Asterisks indicate a statistically significant decrease of phage concentration
691 (PFU/mL) in relation to control cells (Two-way ANOVA, $p < 0.05$). The bars represent
692 the average of two biological replicates, with individual data points overlaid. Images

are representatives of phage mutant T3 n.2 infecting cells at a decreasing phage concentration.

Figure 4. Kiwa reduces phage DNA replication via a RecBCD-dependent mechanism. a Effect of Kiwa on phage absorption to *E. coli* cells. The percentage of phages adsorbed to cells after 15 min was calculated relative to the total amount of phage. The bar graphs show the mean of three biological replicates with individual points overlaid. **b** Quantification of intra- and extracellular phages on cultures of *E. coli* expressing Kiwa ECOR8 or a control. Data shows plaque forming units (PFU/mL) of phage T4 at 90 minutes post infection. Asterisks indicate a statistically significant decrease of PFU compared to control cells (Two-way ANOVA, $p < 0.05$). The bars shows the mean of three biological replicates, with individual data points overlaid. **c** Efficiency of phage DNA replication during infection of control and Kiwa cells. Total DNA was extracted from cells infected with phage at an MOI of 3. The data represents the replication efficiency of phage DNA per minute over 30 minutes of infection, compared to control cells, and is shown as the mean of two biological replicates, with individual data points overlaid. **d** Effect of Kiwa on total ATP levels during phage infection. Data represents ratio of total ATP levels of cells expressing Kiwa relative to the control. Cells where either kept uninfected or infected with phage T3 or T4 at an MOI of 3 or 0.03. Asterisks indicate a statistically significant decrease of ATP in relation to uninfected cells at the same time point (Two-way ANOVA, $p < 0.05$). The bars show the average of two biological replicates with individual data points overlaid. **e** Effect of deleting Kiwa genes on total ATP levels during phage infection. **f** Effect of deleting RecBCD subunits on Kiwa defence. Data represents PFU/mL of phage T4 infecting control or Kiwa cells. Asterisks indicate a statistically

significant decrease of PFU in relation to control cells with complete RecBCD (Two-way ANOVA, $p < 0.01$). The bars show the average of two biological replicates, with individual data points overlaid. **g** Effect of the deletion of RecD on total ATP levels during phage infection. Data represents ratio of total ATP levels of Kiwa cells with or without RecD relative to the control (no defence). Cells where either kept uninfected or infected with phage T3 or T4 at an MOI of 3. Asterisks indicate a statistically significant decrease of ATP compared to uninfected cells at the same time point (Two-way ANOVA, $p < 0.01$). The bars show the average of two replicates, with individual data points overlaid. **h** Effect of deleting RecBCD subunits on KwaB defence activity. Data represents PFU/mL of phage T4 infecting control or ECOR8 KwaB (ΔKwaA) cells with a complete RecBCD complex or single subunit deletions. Asterisks indicate a statistically significant decrease of PFU compared to complete RecBCD expressing cells (Two-way ANOVA, $p < 0.01$). The bars show the average of two biological replicates, with individual data points overlaid. **i** A model for the mechanism of the Kiwa defence system. Phage infection is sensed by the inhibition of the host RNA polymerase by phage proteins, leading to an ATP depletion event that causes the release and activation of KwaB, likely via oligomerisation. The active KwaB re-activates RecBCD, leading to a decrease in phage DNA replication to control the spread of the infection.

Supplementary data

Supplementary Fig. 1: Distribution of Kiwa homologues in bacterial genomes and their anti-phage activity.

Supplementary Fig. 2: Anti-phage activity of modified Kiwa systems from *E. coli* ECOR8 and SN82F48.

Supplementary Fig. 3: KwaB oligomerisation and conservation.

Supplementary Fig. 4: *E. coli* ECOR8c has increased defence against phage infection.

Supplementary Fig. 5: Mutant phage challenges of Kiwa cells expressing phage proteins in *trans*.

Supplementary Fig. 6: The effect of RecBCD and KwaB on Kiwa defence.

Supplementary Table 1: Mutation analysis of bacterial strains and phage escape mutants.

Supplementary Table 2: Strains and phages used in this study.

Supplementary Table 3: Primers and gblocks used in this study.

Supplementary Table 4: Plasmids used in this study.

Supplementary Table 5: Kiwa homologues used for hierarchical clustering.

References

1 Anzalone, A. V., Koblan, L. W. & Liu, D. R. Genome editing with CRISPR–Cas nucleases, base editors, transposases and prime editors. *Nat Biotechnol* **38**, 824-844, doi:10.1038/s41587-020-0561-9 (2020).

2 Millman, A. *et al.* An expanding arsenal of immune systems that protect bacteria from phages. *bioRxiv*, doi:10.1101/2022.05.11.491447 (2022).

3 Doron, S. *et al.* Systematic discovery of antiphage defense systems in the microbial pangenome. *Science* **359**, eaar4120, doi:10.1126/science.aar4120 (2018).

4 Ofir, G. *et al.* DISARM is a widespread bacterial defence system with broad anti-phage activities. *Nat Microbiol* **3**, 90-98, doi:10.1038/s41564-017-0051-0 (2018).

5 Goldfarb, T. *et al.* BREX is a novel phage resistance system widespread in microbial genomes. *EMBO J* **34**, 169-183, doi:10.15252/embj.201489455 (2015).

6 Gao, L. *et al.* Diverse enzymatic activities mediate antiviral immunity in prokaryotes. *Science* **369**, 1077-1084, doi:10.1126/science.aba0372 (2020).

7 Owen, S. V. *et al.* Prophages encode phage-defense systems with cognate self-immunity. *Cell Host Microbe* **29**, 1620-1633.e1628, doi:10.1016/j.chom.2021.09.002 (2021).

8 Rousset, F. *et al.* Phages and their satellites encode hotspots of antiviral systems. *Cell Host Microbe* **30**, 740-753.e745, doi:10.1016/j.chom.2022.02.018 (2022).

9 Vassallo, C. N., Doering, C. R., Littlehale, M. L., Teodoro, G. I. C. & Laub, M. T. A functional selection reveals previously undetected anti-phage defence systems in the E. coli pangenome. *Nat Microbiol* **7**, 1568-1579, doi:10.1038/s41564-022-01219-4 (2022).

10 Payne, L. J. *et al.* Identification and classification of antiviral defence systems in bacteria and archaea with PADLOC reveals new system types. *Nucleic Acids Res* **49**, 10868-10878, doi:10.1093/nar/gkab883 (2021).

11 Isaev, A. *et al.* Phage T7 DNA mimic protein Ocr is a potent inhibitor of BREX defence. *Nucleic Acids Res* **48**, 5397-5406, doi:10.1093/nar/gkaa290 (2020).

12 Gordeeva, J. *et al.* BREX system of Escherichia coli distinguishes self from non-self by methylation of a specific DNA site. *Nucleic Acids Res* **47**, 253-265, doi:10.1093/nar/gky1125 (2018).

13 Bravo, J. P. K., Aparicio-Maldonado, C., Nobrega, F. L., Brouns, S. J. J. & Taylor, D. W. Structural basis for broad anti-phage immunity by DISARM. *Nat Commun* **13**, 2987, doi:10.1038/s41467-022-30673-1 (2022).

14 Aparicio-Maldonado, C. *et al.* Class I DISARM provides anti-phage and anti-conjugation activity by unmethylated DNA recognition. *bioRxiv*, doi:10.1101/2021.12.28.474362 (2021).

15 Duncan-Lowey, B., McNamara-Bordewick, N. K., Tal, N., Sorek, R. & Kranzusch, P. J. Effector-mediated membrane disruption controls cell death in CBASS antiphage defense. *Mol Cell* **81**, 5039-5051.e5035, doi:10.1016/j.molcel.2021.10.020 (2021).

16 Cohen, D. *et al.* Cyclic GMP–AMP signalling protects bacteria against viral infection. *Nature* **574**, 691-695, doi:10.1038/s41586-019-1605-5 (2019).

17 Ofir, G. *et al.* Antiviral activity of bacterial TIR domains via signaling molecules that trigger cell death. *bioRxiv*, doi:10.1101/2021.01.06.425286 (2021).

18 Ka, D., Oh, H., Park, E., Kim, J.-H. & Bae, E. Structural and functional evidence of bacterial antiphage protection by Thoeris defense system via NAD+ degradation. *Nat Commun* **11**, 2816, doi:10.1038/s41467-020-16703-w (2020).

19 Tal, N. *et al.* Cyclic CMP and cyclic UMP mediate bacterial immunity against phages. *Cell* **184**, 5728-5739.e5716, doi:10.1016/j.cell.2021.09.031 (2021).

20 Cheng, R. *et al.* The prokaryotic Gabija complex senses both viral transcription and DNA metabolism for antiviral defense. Research Square, doi: 10.21203/rs.3.rs-1703025/v1 (2022).

21 Cheng, R. *et al.* A nucleotide-sensing endonuclease from the Gabija bacterial defense system. *Nucleic Acids Res* **49**, 5216-5229, doi:10.1093/nar/gkab277 (2021).

22 Millman, A. *et al.* Bacterial Retrons Function In Anti-Phage Defense. *Cell* **183**, 1551-1561.e1512, doi:10.1016/j.cell.2020.09.065 (2020).

23 Gao, Y. *et al.* Molecular basis of RADAR anti-phage supramolecular assemblies. *Cell*, doi:10.1016/j.cell.2023.01.026 (2023).

24 Duncan-Lowey, B. *et al.* Cryo-EM structure of the RADAR supramolecular anti-phage defense complex. *Cell*, doi:10.1016/j.cell.2023.01.012 (2023).

25 Garb, J. *et al.* Multiple phage resistance systems inhibit infection via SIR2-dependent NAD+ depletion. *Nat Microbiol* **7**, 1849-1856, doi:10.1038/s41564-022-01207-8 (2022).

26 Gao, L. A. *et al.* Prokaryotic innate immunity through pattern recognition of conserved viral proteins. *Science* **377**, eabm4096, doi:10.1126/science.abm4096 (2022).

27 Johnson, A. G. *et al.* Bacterial gasdermins reveal an ancient mechanism of cell death. *Science* **375**, 221-225, doi:10.1126/science.abj8432 (2022).

28 Hsueh, B. Y. *et al.* Phage defence by deaminase-mediated depletion of deoxynucleotides in bacteria. *Nat Microbiol* **7**, 1210-1220, doi:10.1038/s41564-022-01162-4 (2022).

29 Tal, N. *et al.* Bacteria deplete deoxynucleotides to defend against bacteriophage infection. *Nat Microbiol* **7**, 1200-1209, doi:10.1038/s41564-022-01158-0 (2022).

30 Bernheim, A. *et al.* Prokaryotic viperins produce diverse antiviral molecules. *Nature* **589**, 120-124, doi:10.1038/s41586-020-2762-2 (2021).

31 Cuozzo, S. A., Sesma, F., Palacios, J. M., de Ruíz Holgado, A. d. P. & Raya, R. R. Identification and nucleotide sequence of genes involved in the synthesis of lactocin 705, a two-peptide bacteriocin from Lactobacillus casei CRL 705. *FEMS Microbiol Let* **185**, 157-161, doi:10.1016/S0378-1097(00)00093-8 (2000).

32 Jumper, J. *et al.* Highly accurate protein structure prediction with AlphaFold. *Nature* **596**, 583-589, doi:10.1038/s41586-021-03819-2 (2021).

33 Florea, M. *et al.* Engineering control of bacterial cellulose production using a genetic toolkit and a new cellulose-producing strain. *Proc Natl Acad Sci U S A* **113**, E3431-E3440, doi:10.1073/pnas.1522985113 (2016).

34 Lopatina, A., Tal, N. & Sorek, R. Abortive Infection: Bacterial Suicide as an Antiviral Immune Strategy. *Ann Rev Virol* **7**, 371-384, doi:10.1146/annurev-virology-011620-040628 (2020).

35 Stokar-Avihail, A. *et al.* Discovery of phage determinants that confer sensitivity to bacterial immune systems. *bioRxiv*, doi:10.1101/2022.08.27.505566 (2022).

36 Tabib-Salazar, A. *et al.* T7 phage factor required for managing RpoS in Escherichia coli. *Proc Natl Acad Sci U S A* **115**, E5353-E5362, doi:10.1073/pnas.1800429115 (2018).

37 Tabib-Salazar, A. *et al.* Full shut-off of Escherichia coli RNA-polymerase by T7 phage requires a small phage-encoded DNA-binding protein. *Nucleic Acids Res* **45**, 7697-7707, doi:10.1093/nar/gkx370 (2017).

38 Schmitt, C. K., Kemp, P. & Molineux, I. J. Genes 1.2 and 10 of bacteriophages T3 and T7 determine the permeability lesions observed in infected cells of Escherichia coli expressing the F plasmid gene pifA. *J Bacteriol* **173**, 6507-6514, doi:10.1128/jb.173.20.6507-6514.1991 (1991).

39 Parma, D. H. *et al.* The Rex system of bacteriophage lambda: tolerance and altruistic cell death. *Genes Dev* **6**, 497-510, doi:10.1101/gad.6.3.497 (1992).

40 Cheng, X., Wang, W. & Molineux, I. J. F exclusion of bacteriophage T7 occurs at the cell membrane. *Virology* **326**, 340-352, doi:10.1016/j.virol.2004.06.001 (2004).

41 Millman, A., Melamed, S., Amitai, G. & Sorek, R. Diversity and classification of cyclic-oligonucleotide-based anti-phage signalling systems. *Nat Microbiol* **5**, 1608-1615, doi:10.1038/s41564-020-0777-y (2020).

42 Cecchini, N., Schmerer, M., Molineux, I. J., Springman, R. & Bull, J. J. Evolutionarily Stable Attenuation by Genome Rearrangement in a Virus. *G3 Gene Genome Genet* **3**, 1389-1397, doi:10.1534/g3.113.006403 (2013).

43 Dillingham, M. S. & Kowalczykowski, S. C. RecBCD Enzyme and the Repair of Double-Stranded DNA Breaks. *Microbiol Mol Biol Rev* **72**, 642-671, doi:10.1128/MMBR.00020-08 (2008).

44 Cheng, K., Wilkinson, M., Chaban, Y. & Wigley, D. B. A conformational switch in response to Chi converts RecBCD from phage destruction to DNA repair. *Nat Struct Mol Biol* **27**, 71-77, doi:10.1038/s41594-019-0355-2 (2020).

45 Levy, A. *et al.* CRISPR adaptation biases explain preference for acquisition of foreign DNA. *Nature* **520**, 505-510, doi:10.1038/nature14302 (2015).

46 Kuzmenko, A. *et al.* pAgo-induced DNA interference protects bacteria from invader DNA. *bioRxiv*, doi:10.1101/2020.03.01.971358 (2020).

47 Chen, H.-W., Randle, D. E., Gabbidon, M. & Julin, D. A. Functions of the ATP hydrolysis subunits (RecB and RecD) in the nuclease reactions catalyzed by

the RecBCD enzyme fromEscherichia coli11Edited by G. Smith. *J Mol Biol* **278**, 89-104, doi:10.1006/jmbi.1998.1694 (1998).

48 Guegler, C. K. & Laub, M. T. Shutoff of host transcription triggers a toxin-antitoxin system to cleave phage RNA and abort infection. *Mol Cell* **81**, 2361-2373.e2369, doi:10.1016/j.molcel.2021.03.027 (2021).

49 Zabrady, K., Zabrady, M., Kolesar, P., Li, A. W. H. & Doherty, A. J. CRISPR-Associated Primase-Polymerases are implicated in prokaryotic CRISPR-Cas adaptation. *Nat Commun* **12**, 3690, doi:10.1038/s41467-021-23535-9 (2021).

50 Kutter, E. *et al.* From Host to Phage Metabolism: Hot Tales of Phage T4's Takeover of E. coli. *Viruses* **10**, 387 (2018).

51 Krüger, D. H. & Schroeder, C. Bacteriophage T3 and bacteriophage T7 virus-host cell interactions. *Microbiol Rev* **45**, 9-51, doi:10.1128/mr.45.1.9-51.1981 (1981).

52 Li, H. Minimap2: pairwise alignment for nucleotide sequences. *Bioinformatics* **34**, 3094-3100, doi:10.1093/bioinformatics/bty191 (2018).

53 Luong, T., Salabarria, A.-C., Edwards, R. A. & Roach, D. R. Standardized bacteriophage purification for personalized phage therapy. *Nat Prot* **15**, 2867-2890, doi:10.1038/s41596-020-0346-0 (2020).

54 Deatherage, D. E. & Barrick, J. E. in *Engineering and Analyzing Multicellular Systems: Methods and Protocols* (eds Lianhong Sun & Wenying Shou) 165-188 (Springer New York, 2014).

55 Pabst, M. *et al.* A general approach to explore prokaryotic protein glycosylation reveals the unique surface layer modulation of an anammox bacterium. *ISME J* **16**, 346-357, doi:10.1038/s41396-021-01073-y (2022).

56 Sievers, F. *et al.* Fast, scalable generation of high-quality protein multiple sequence alignments using Clustal Omega. *Mol Sys Biol* **7**, 539, doi:10.1038/msb.2011.75 (2011).

57 Tumescheit, C., Firth, A. & Brown, K. CIAlign: A highly customisable command line tool to clean, interpret and visualise multiple sequence alignments. *PeerJ* **10**, e12983 (2022).

58 Nguyen, L.-T., Schmidt, H. A., von Haeseler, A. & Minh, B. Q. IQ-TREE: A Fast and Effective Stochastic Algorithm for Estimating Maximum-Likelihood Phylogenies. *Mol Biol Evol* **32**, 268-274, doi:10.1093/molbev/msu300 (2014).

59 Letunic, I. & Bork, P. Interactive Tree Of Life (iTOL) v4: recent updates and new developments. *Nucleic Acids Res* **47**, W256-W259, doi:10.1093/nar/gkz239 (2019).

60 Söding, J., Biegert, A. & Lupas, A. N. The HHpred interactive server for protein homology detection and structure prediction. *Nucleic Acids Res* **33**, W244-W248, doi:10.1093/nar/gki408 (2005).

61 Hallgren, J. *et al.* DeepTMHMM predicts alpha and beta transmembrane proteins using deep neural networks. *bioRxiv*, doi:10.1101/2022.04.08.487609 (2022).

62 Gasteiger, E. *et al.* in *The Proteomics Protocols Handbook* (ed John M. Walker) 571-607 (Humana Press, 2005).

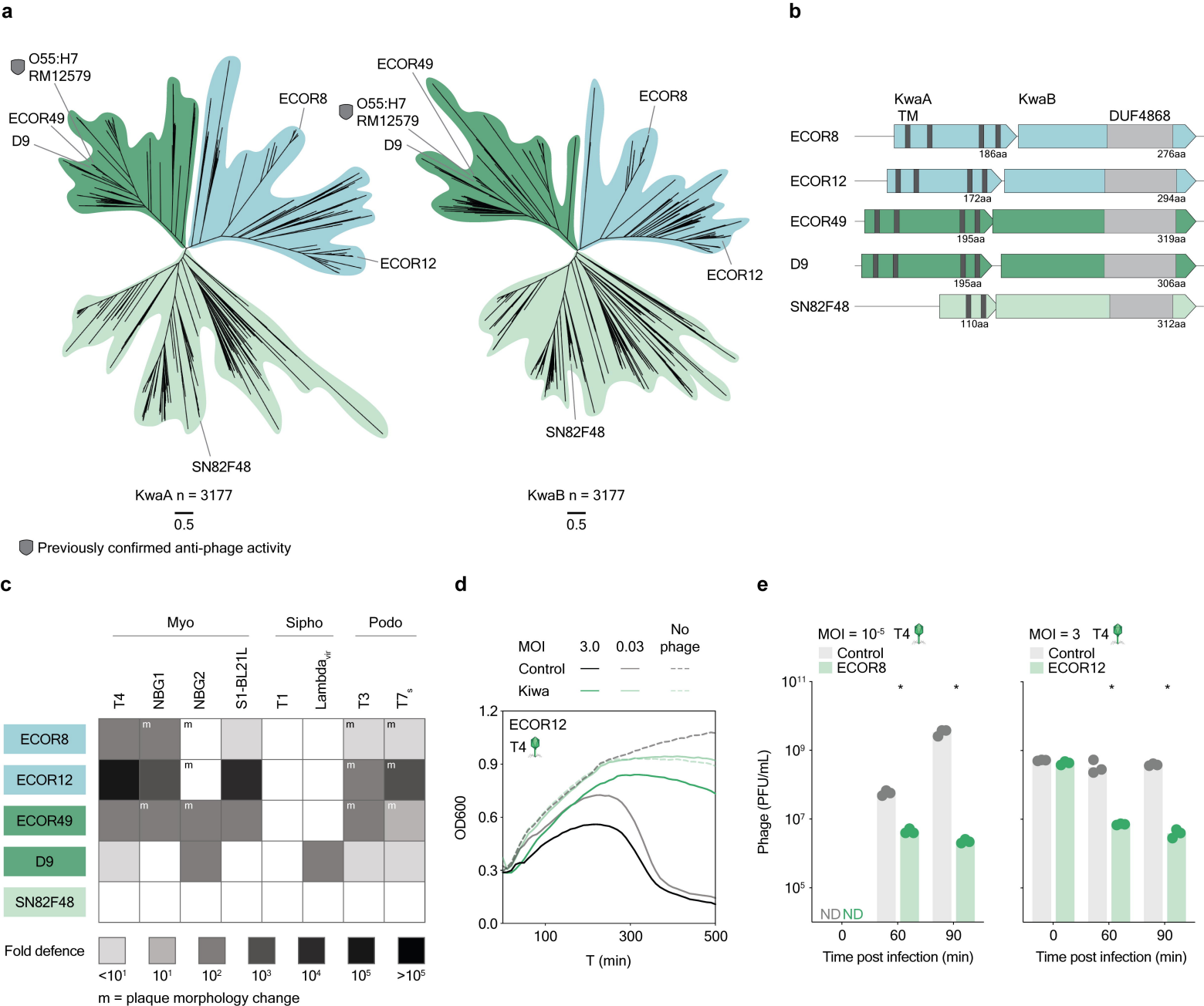
a
O55:H7
RM12579
ECOR49
D9
ECOR8
ECOR12
SN82F48
KwaA n = 3177
0.5
ECOR49
O55:H7
RM12579
D9
ECOR8
ECOR12
SN82F48
KwaB n = 3177
0.5
Previously confirmed anti-phage activity
b
KwaA
TM
KwaB
DUF4868
ECOR8
186aa
276aa
ECOR12
172aa
294aa
ECOR49
195aa
319aa
D9
195aa
306aa
SN82F48
110aa
312aa
c
Myo
Sipho
Podo
T4
NBG1
NBG2
S1-BL21L
T1
Lambda$_{vir}$
T3
T7$_s$
ECOR8
ECOR12
ECOR49
D9
SN82F48
Fold defence
<10^1
10^1
10^2
10^3
10^4
10^5
>10^5
m = plaque morphology change
d
MOI
3.0
0.03
No phage
Control
Kiwa
ECOR12
T4
OD600
T (min)
e
MOI = 10^{-5} T4
Control
ECOR8
MOI = 3 T4
Control
ECOR12
Phage (PFU/mL)
ND
ND
Time post infection (min)
Time post infection (min)

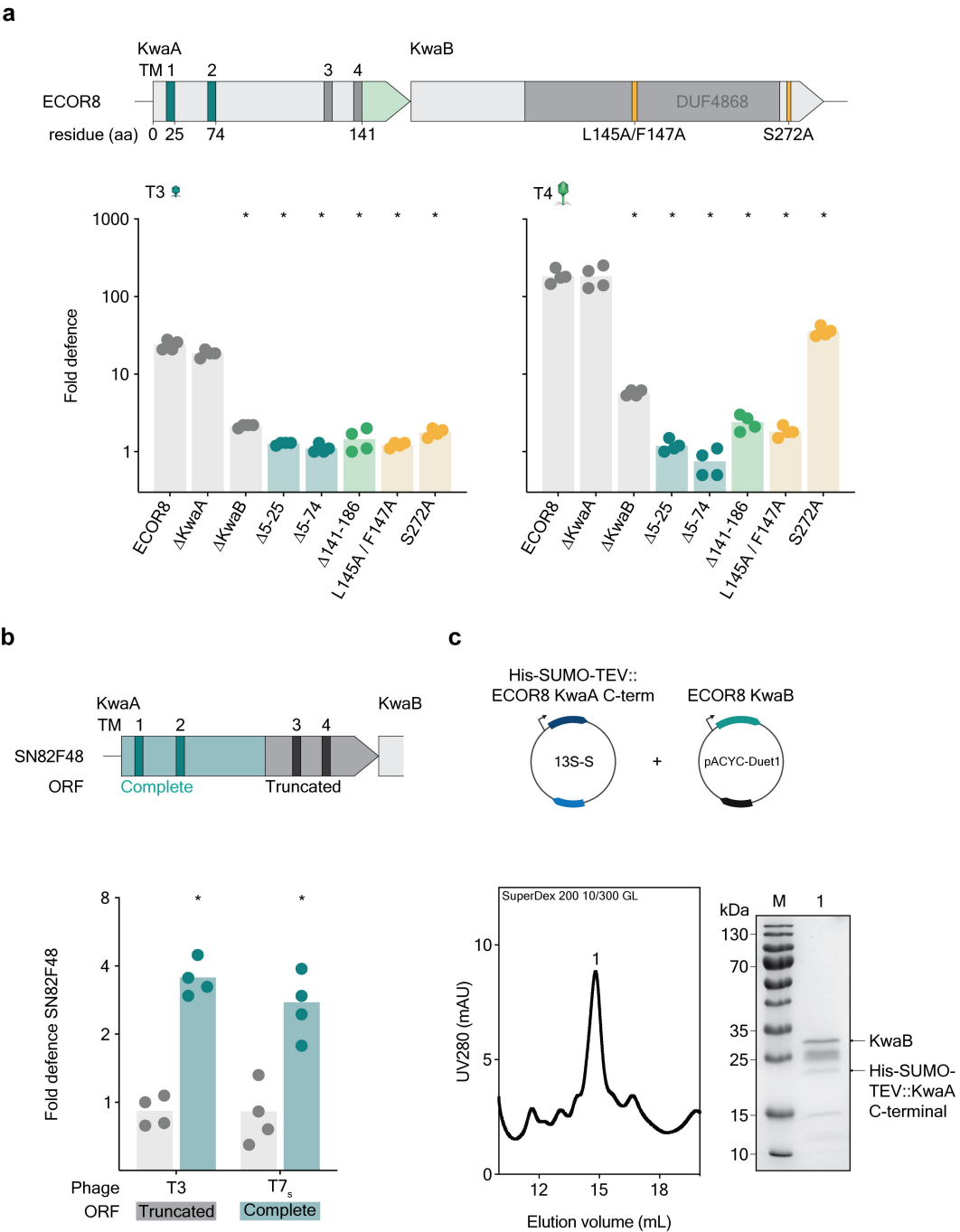
a
KwaA
TM 1
2
3
4
KwaB
ECOR8
DUF4868
residue (aa) 0 25 74 141 L145A/F147A S272A
T3
T4
Fold defence
1000
100
10
1
ECOR8
ΔKwaA
ΔKwaB
Δ5-25
Δ5-74
Δ141-186
L 145A / F147A
S272A
b
KwaA
TM 1 2 3 4
KwaB
SN82F48
ORF
Complete
Truncated
Fold defence SN82F48
8
4
2
1
Phage
T3
T7s
ORF
Truncated
Complete
c
His-SUMO-TEV::
ECOR8 KwaA C-term
ECOR8 KwaB
13S-S
+
pACYC-Duet1
SuperDex 200 10/300 GL
UV280 (mAU)
10
5
0
1
12
15
18
Elution volume (mL)
kDa
M
1
130
70
35
25
15
10
KwaB
His-SUMO-
TEV::KwaA
C-terminal

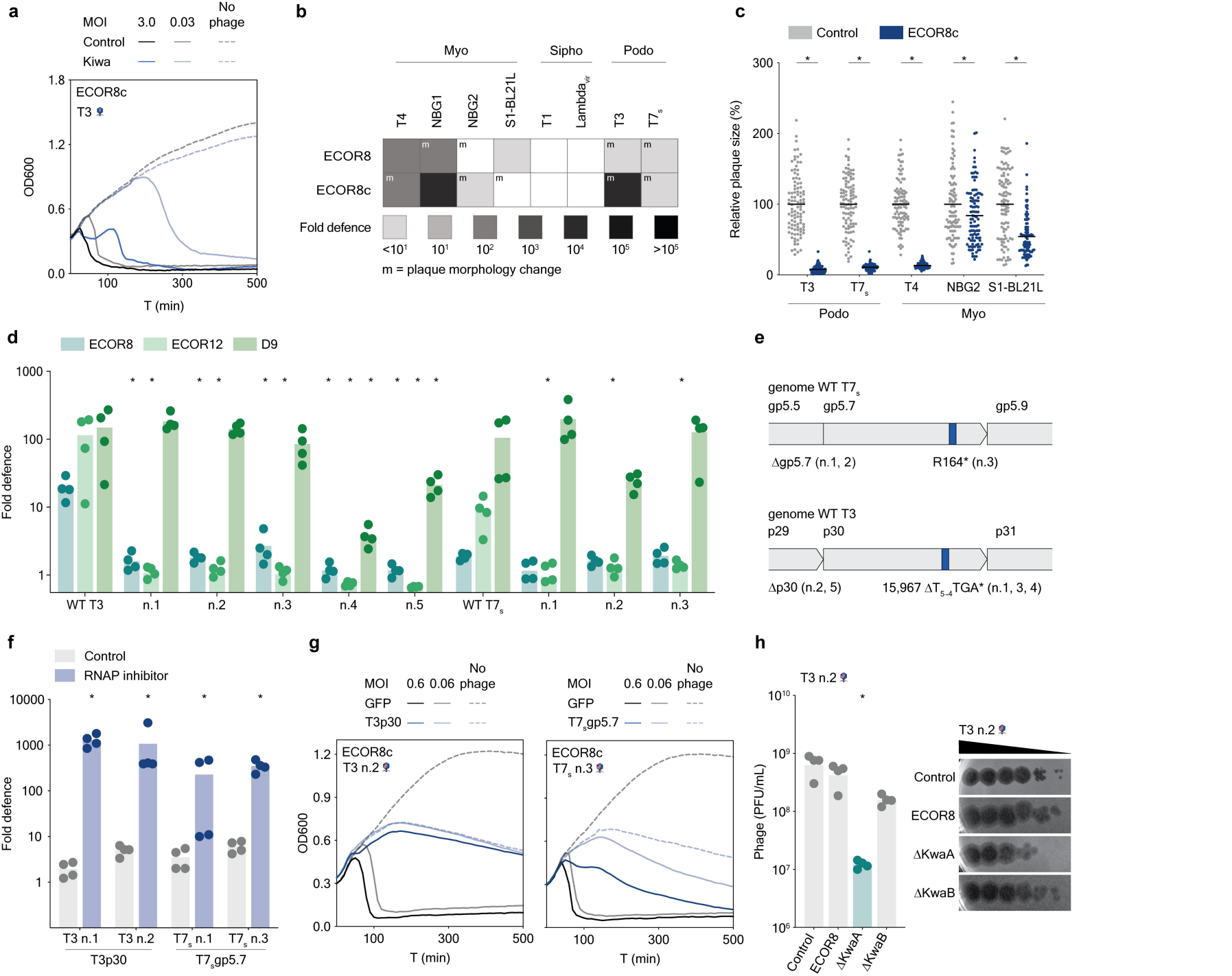
a
MOI 3.0 0.03 No phage
Control
Kiwa
ECOR8c
T3
OD600
T (min)
b
Myo
Sipho
Podo
T4
NBG1
NBG2
S1-BL21L
T1
Lambda vir
T3
T7s
ECOR8
ECOR8c
Fold defence
<10¹ 10¹ 10² 10³ 10⁴ 10⁵ >10⁵
m = plaque morphology change
c
Control
ECOR8c
Relative plaque size (%)
T3
T7s
T4
NBG2
S1-BL21L
Podo
Myo
d
ECOR8
ECOR12
D9
Fold defence
WT T3
n.1
n.2
n.3
n.4
n.5
WT T7s
e
genome WT T7s
gp5.5
gp5.7
gp5.9
Δgp5.7 (n.1, 2)
R164* (n.3)
genome WT T3
p29
p30
p31
Δp30 (n.2, 5)
15,967 ΔT5-4TGA* (n.1, 3, 4)
f
Control
RNAP inhibitor
Fold defence
T3 n.1
T3 n.2
T7s n.1
T7s n.3
T3p30
T7sgp5.7
g
MOI 0.6 0.06 No phage
GFP
T3p30
T7sgp5.7
ECOR8c
T3 n.2
T7s n.3
OD600
T (min)
h
T3 n.2
Phage (PFU/mL)
Control
ECOR8
ΔKwaA
ΔKwaB

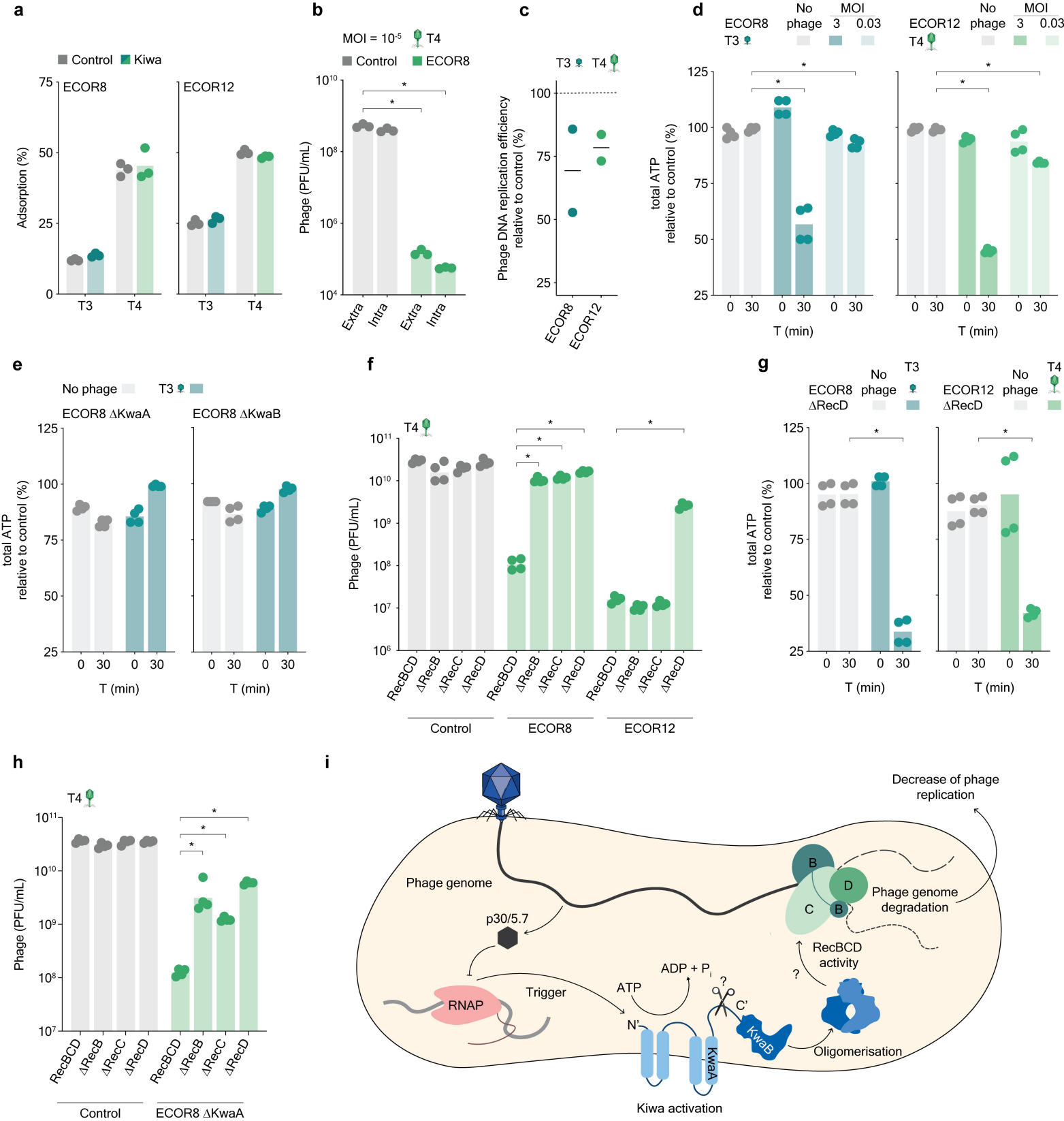
a
Control
Kiwa
ECOR8
ECOR12
Adsorption (%)
T3
T4
b
MOI = 10-5
T4
Control
ECOR8
Phage (PFU/mL)
Extra
Intra
c
T3
T4
Phage DNA replication efficiency relative to control (%)
ECOR8
ECOR12
d
ECOR8
T3
No phage
MOI
3
0.03
ECOR12
T4
total ATP relative to control (%)
T (min)
e
No phage
T3
ECOR8 ΔKwaA
ECOR8 ΔKwaB
total ATP relative to control (%)
T (min)
f
T4
Phage (PFU/mL)
RecBCD
ΔRecB
ΔRecC
ΔRecD
Control
ECOR8
ECOR12
g
ECOR8
ΔRecD
No phage
T3
ECOR12
ΔRecD
No phage
T4
total ATP relative to control (%)
T (min)
h
T4
Phage (PFU/mL)
RecBCD
ΔRecB
ΔRecC
ΔRecD
Control
ECOR8 ΔKwaA
i
Decrease of phage replication
Phage genome
p30/5.7
Trigger
RNAP
ATP
ADP + Pi
N'
C'
KwaA
KwaB
Kiwa activation
Oligomerisation
RecBCD activity
Phage genome degradation
B
D
C
B